The Palladium(II)-Substituted, Lone Pair Containing Tungstoarsenates(III) $[Na_2(H_2O)_2PdWO(H_2O)(\alpha\text{-}AsW_9O_{33})_2]^{10-}$ and $[Cs_2Na(H_2O)_8Pd_3(\alpha\text{-}AsW_9O_{33})_2]^{9-}$

Li-Hua Bi,[a] Ulrich Kortz,*[a] Bineta Keita,[b] Louis Nadjo,[b] and Lee Daniels[c]

Keywords: Arsenic / Crystal structure / Electrochemistry / Palladium / Polyoxometalates / Tungsten

The monopalladium(II)-substituted $[Na_2(H_2O)_2PdWO(H_2O)(\alpha\text{-}AsW_9O_{33})_2]^{10-}$ (**1**) and the tripalladium(II)-substituted $[Cs_2Na(H_2O)_8Pd_3(\alpha\text{-}AsW_9O_{33})_2]^{9-}$ (**2**) were synthesized in aqueous acidic medium (pH 4.8) by reaction of Pd^{2+} ions with $[As_2W_{19}O_{67}(H_2O)]^{14-}$ and $[\alpha\text{-}AsW_9O_{33}]^{9-}$, respectively. The dimeric polyanions **1** and **2** were characterized by complete elemental analysis, FTIR, and electrochemistry. Single-crystal X-ray analysis was carried out on $Cs_3Na_7[Na_2(H_2O)_2PdWO(H_2O)(\alpha\text{-}AsW_9O_{33})_2]\cdot 1.5NaCl\cdot 22H_2O$ (**1a**), which crystallizes in the triclinic system, space group $P\bar{1}$, with a = 13.2465(16) Å, b = 16.873(2) Å, c = 23.080(3) Å, α = 107.315(2)°, β = 95.025(3)°, γ = 98.040(3)°, and Z = 2; $Cs_3Na_6[Cs_2Na(H_2O)_8Pd_3(\alpha\text{-}AsW_9O_{33})_2]\cdot NaCl\cdot 15H_2O$ (**2a**) crystallizes in the monoclinic system, space group $P2_1/m$, with a = 13.1842(5) Å, b = 19.6584(7) Å, c = 18.2377(6) Å, β = 100.7660(10)°, and Z = 2. Polyanion **1** is composed of two $[\alpha\text{-}AsW_9O_{33}]^{9-}$ fragments connected by a $WO(H_2O)$ unit, one square-planar palladium atom and two sodium ions, leading to a sandwich-type structure with C_s symmetry. Polyanion **2** also consists of two $[\alpha\text{-}AsW_9O_{33}]^{9-}$ moieties, but these are linked by three equivalent, square-planar Pd^{2+} ions, one sodium ion and two cesium ions, leading to a sandwich-type structure with C_{2v} symmetry. A cyclic voltammetric study of polyanion **2** in a pH 5 medium shows a Pd^0 deposition process on the glassy carbon electrode surface. The corresponding wave and the waves for the tungsten redox processes could be separated clearly. The thickness of the film increases with the number of potential cycles or the duration of potentiostatic electrolysis. The deposited film proved to be very stable and efficient in the electrocatalytic reduction of dioxygen. Polyanion **1** was not sufficiently stable in solution to warrant electrochemical characterization.

Introduction

Polyoxometalates (POMs) are a well-known class of metal–oxygen cluster species with a diverse compositional range and structural variety, and therefore, they attract increasing attention worldwide.[1] Although POMs have been known for about 200 years, a large number of novel polyoxoanions with different size, composition and structure are still being discovered.[2–4] The fascinating properties of POMs allow to envisage applications in different fields including catalysis, medicine and materials science.[5–7] Therefore, systematic structural design of novel POMs and derivatization of known POMs continue to be a considerable focus in the ongoing research in POM chemistry. Most POMs are composed of early transition metal MO_6 ($M = W^{6+}$, Mo^{6+}, etc.) octahedra and main group XO_4 ($X = P^V$, Si^{IV}, etc.) tetrahedra. The most famous POMs are probably the Keggin (e.g. $PW_{12}O_{40}^{3-}$) and the Wells–Dawson (e.g. $P_2W_{18}O_{62}^{6-}$) ions.[2]

The existence of As^{III}-containing POMs has been known for several years.[8] The lone pair of electrons on the heteroatom does not allow the closed Keggin unit to form, which has resulted in some unexpected structures, e.g. $[NH_4As_4W_{40}O_{140}Co_2(H_2O)_2]^{23-}$, $[As_4W_{20}O_{72}(H_2O)_2]^{12-}$, $[H_2AsW_{18}O_{60}]^{7-}$, and $[AsW_8O_{30}AsOH]^{7-}$.[9] A few years ago, Pope et al. reported on $[As_{12}Ce_{16}(H_2O)_{36}W_{148}O_{524}]^{76-}$, which also is the largest polyoxotungstate known to date.[10] This supramolecular polyanion is composed of 12 (α-AsW_9O_{33}) and four (W_5O_{18}) units. More recently, Kortz et al. reported on the second largest tungstoarsenate known to date, $[As_6W_{65}O_{217}(H_2O)_7]^{26-}$.[11] This species consists of four inner (β-AsW_9O_{33}) and two outer (α-AsW_9O_{33}) fragments that are linked by a total of 11 corner-sharing WO_6 octahedra.

The nonatungstoarsenate(III) $[\alpha\text{-}AsW_9O_{33}]^{9-}$ was discovered by Tourné et al. in 1973,[8a] and since then, the interaction of this trivacant ligand with transition-metal ions has been studied. Such work has resulted predominantly in di-

[a] International University Bremen, School of Engineering and Science,
P. O. Box 750 561, 28725 Bremen, Germany
Fax: +49-421-200-3229
E-mail: u.kortz@iu-bremen.de
[b] Laboratoire de Chimie Physique, UMR 8000,
CNRS, Equipe d'Electrochimie et Photoélectrochimie, Université Paris-Sud, Bâtiment 420,
91405 Orsay Cedex, France
[c] Rigaku/MSC,
9009 New Trails Drive, The Woodlands, Texas 77381-5209, USA

  DOI: 10.1002/ejic.200500128

meric, sandwich-type structures, and the first member of this class ($[Cu_3(H_2O)_2(\alpha\text{-}AsW_9O_{33})_2]^{12-}$) was reported by Hervé et al. in 1982.[12] Since then a number of isostructural derivatives have been characterized: $[M_3(H_2O)_3(\alpha\text{-}AsW_9O_{33})_2]^{12-}$ (M = Mn^{2+}, Co^{2+}, Ni^{2+}, Cu^{2+}, Zn^{2+}) and $[(VO)_3(\alpha\text{-}AsW_9O_{33})_2]^{11-}$.[13] Very recently, Kortz et al. described the first example of a sandwich-type species with four transition metals, $[Cu_4K_2(H_2O)_8(\alpha\text{-}AsW_9O_{33})_2]^{8-}$.[14] Recently, tetrasubstituted sandwich-type POMs based on the $[\beta\text{-}AsW_9O_{33}]^{9-}$ fragment have also been reported, e.g. $[M_4(H_2O)_{10}(\beta\text{-}AsW_9O_{33})_2]^{6-}$ (M = Fe^{3+}, Cr^{3+}).[15]

The 19-tungstodiarsenate(III) $[As_2W_{19}O_{67}(H_2O)]^{14-}$ was also reported by Tourné et al. in 1973,[8a] and its structure was recently confirmed by Kortz and coworkers.[11] This polyanion consists of two $[\alpha\text{-}AsW_9O_{33}]^{9-}$ fragments, which are linked by an additional tungsten center, resulting in a dilacunary species. The interaction of $[As_2W_{19}O_{67}(H_2O)]^{14-}$ with di- and trivalent transition-metal and main-group elements has been investigated by different groups and has resulted in disubstituted products $[M_2As_2W_{19}O_{67}(H_2O)_3]^{n-}$ (n = 10, M = Mn^{2+}, Co^{2+}, Ni^{2+}, Cu^{2+}, Zn^{2+}, VO^{2+}; n = 8, M = Mn^{3+}, Fe^{3+}, Ga^{3+}).[13a, 16]

The 20-tungstodiarsenate(III) $[As_2W_{20}O_{68}(H_2O)]^{10-}$ was first reported by Hervé et al. who synthesized this as a monolacunary species from the dilacunary precursor $[As_2W_{19}O_{67}(H_2O)]^{14-}$.[17] The same authors also studied the interaction of $[As_2W_{20}O_{68}(H_2O)]^{10-}$ with first-row transition-metal ions, which leads to the monosubstituted products $[MAs_2W_{20}O_{68}(H_2O)_2]^{8-}$ (M = Mn^{2+}, Co^{2+}, Ni^{2+}, Cu^{2+}, Zn^{2+}, VO^{2+}).[17] Recently, Kortz et al. reported on the ytterbium derivative $[YbAs_2W_{20}O_{68}(H_2O)_3]^{7-}$.[18]

All of the above sandwich-type structures can be considered to be derivatives of Jeannin's 21-tungstodiarsenate(III) $[As_2W_{21}O_{69}(H_2O)]^{6-}$, which consists of two $[\alpha\text{-}AsW_9O_{33}]^{9-}$ fragments linked by a belt of three tungsten atoms.[19]

Organotin-substituted tungstoarsenates(III) of this structural type have also been prepared. Pope et al. reported on tetrasubstituted $[\{C_6H_5Sn)_2O\}_2H(AsW_9O_{33})_2]^{9-}$,[20] and later, Kortz et al. prepared disubstituted $[(C_6H_5Sn)_2As_2W_{19}O_{67}(H_2O)]^{8-}$.[21] Very recently, Kortz et al. synthesized the first diorganotin-substituted tungstoarsenate(III), $[\{Sn(CH_3)_2(H_2O)_2\}_3(\beta\text{-}AsW_9O_{33})]^{3-}$, which self-condenses in the solid state leading to the hybrid organic–inorganic 2D material $(CsNa_2[\{Sn(CH_3)_2\}_3(\beta\text{-}AsW_9O_{33})]\cdot 7H_2O)_\infty$.[22]

For many years, POM researchers have attempted to incorporate 4d and 5d elements, in general, and Pd, in particular, in lacunary POMs because of the highly interesting catalytic properties of such species. For a long time the two Pd^{II}-containing polyoxotungstates $[Pd_3(A\text{-}PW_9O_{34})_2]^{12-}$ [23] and $[WZnPd_2(H_2O)_2(B\text{-}\alpha\text{-}ZnW_9O_{34})_2]^{12-}$ [24] have been the only known members of this class, and both were not structurally characterized by X-ray diffraction. Nevertheless, it has been demonstrated that these POMs have excellent catalytic properties for the selective and efficient transformation of organic substrates.[25] In 1994, Angus–Dunne et al. reported on the synthesis and structure of $[Pd_2W_{10}O_{36}]^{8-}$, which represents the first palladium(II)-substituted isopolytungstate.[26] In 2001, Krebs et al. reported on the structure of the tripalladium-substituted tungstotellurate $[Pd_3(TeW_9O_{33})_2]^{10-}$, but without providing any synthetic or crystallographic details.[6]

Recently, we also engaged in the synthesis of polyoxotungstates substituted by noble metals (e.g. Pd, Ru). We already reported on the two novel $Ru^{II}(dmso)_3$-supported polyanions $[HW_9O_{33}Ru^{II}_2(dmso)_6]^{7-}$ and $[Ru(dmso)_3(H_2O)XW_{11}O_{39}]^{6-}$ (X = Ge, Si).[27] Furthermore, we investigated the possibility of forming the Pd^{II} analogs of our tricopper(II)-substituted derivatives $[Cu_3(H_2O)_3(\alpha\text{-}XW_9O_{33})_2]^{12-}$ (X = As^{III}, Sb^{III}).[13a] This proved to be possible, and very recently, we reported on the synthesis and electrochemistry of the first structurally characterized palladium(II)-substituted heteropolyanion $[Cs_2Na(H_2O)_{10}Pd_3(\alpha\text{-}SbW_9O_{33})_2]^{9-}$.[28] We have also already reported on the structure and electrochemistry of the Pd^{II}-substituted tungstosilicate $[Cs_2K(H_2O)_7Pd_2WO(H_2O)(A\text{-}\alpha\text{-}SiW_9O_{34})_2]^{9-}$.[29]

Here we report on two novel palladium(II)-substituted tungstoarsenates(III).

Results and Discussion

Synthesis and Structure

The novel palladium(II)-substituted, dimeric tungstoarsenate(III) $[Na_2(H_2O)_2PdWO(H_2O)(\alpha\text{-}AsW_9O_{33})_2]^{10-}$ (**1**) has been synthesized by reaction of $PdCl_2$ with $K_{14}[As_2W_{19}O_{67}(H_2O)]$ in aqueous acidic medium and isolated as a mixed cesium–sodium salt. Polyanion **1** represents only the third example of a structurally characterized palladium-substituted heteropolytungstate.[28,29] The sandwich-type **1** consists of two lacunary B-α-$[AsW_9O_{33}]^{9-}$ Keggin fragments linked by a Pd atom and a $WO(H_2O)^{4+}$ moiety, which leads to a structure with nominal C_s symmetry (see Figure 1 and Figure 2). Alternatively, **1** can be described as a $[As_2W_{19}O_{67}(H_2O)]^{14-}$ fragment that has taken up a palladium atom. We originally expected incorporation of two palladium atoms in dilacunary $[As_2W_{19}O_{67}(H_2O)]^{14-}$. However, it is not clear why this precursor picks up only one rather than the expected two palladium centers. Surprisingly, the third addenda atom position in the central belt of **1** is occupied by a sodium ion (Na2). Interestingly, Na2 is five-coordinate and is bonded by four terminal oxo groups [Na2···O 2.24–2.34(2) Å] of the two Keggin units in **1** and another terminal oxo group [Na2···O 2.42(3) Å] of W19, resulting in a square-pyramidal coordination sphere. Only one of the resulting three vacancies between W19, Na2 and the palladium atom is occupied by an additional sodium ion Na1. This Na1 is six-coordinate and is bonded by four bridging oxo groups [Na1···O 2.50–2.52(2) Å] of **1** and two terminal water molecules [Na1···O 2.41–2.48(3) Å] resulting in an octahedral coordination sphere. The orientation of Na1 in the belt of **1** is not all that surprising, as crystal structures of several 3d transition-metal derivatives have also revealed the presence of sodium ions in analogous positions. In the di- and tri-transition-metal-substituted derivatives $[M_2(H_2O)_2WO(H_2O)Na_3(H_2O)_6(\alpha\text{-}AsW_9O_{33})_2]^{7-}$ (M = Co^{2+}, Zn^{2+}, Mn^{2+}) and $[M_3(H_2O)_3Na_3(H_2O)_6(\alpha$-

$AsW_9O_{33})_2]^{9-}$ (M = Mn^{2+}, Co^{2+}, Cu^{2+}, Zn^{2+}), three sodium ions were observed in the central belt in equivalent positions.[13] In the monophenyltin derivative $[(C_6H_5Sn)_2Na(H_2O)_2As_2W_{19}O_{67}(H_2O)]^{7-}$, a sodium ion was found between the two tin atoms.[21] Finally, in Pope's $[(C_6H_5Sn)_3Na_3(H_2O)_6(\alpha\text{-}SbW_9O_{33})_2]^{6-}$, three sodium ions are located in the central belt in addition to the three C_6H_5Sn groups.[20]

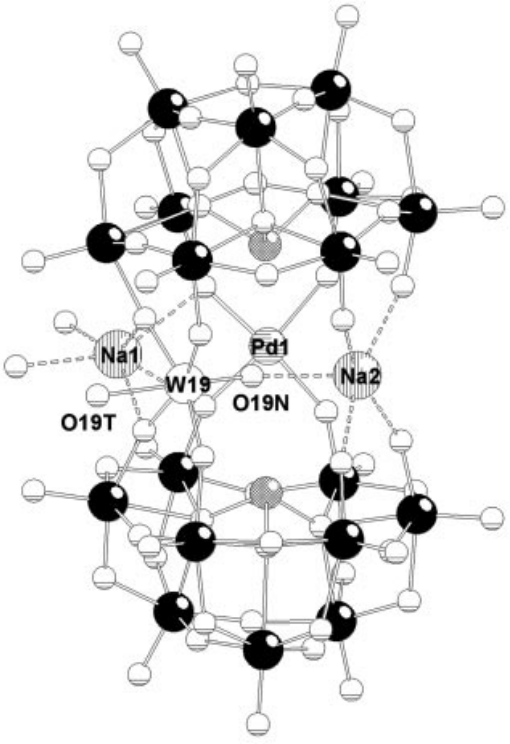

Figure 1. Ball and stick representation of $[Na_2(H_2O)_2PdWO(H_2O)(\alpha\text{-}AsW_9O_{33})_2]^{10-}$ (**1**) showing labels for some selected atoms in the central belt. The shading of the remaining atoms is as follows: tungsten (black), arsenic (cross-hatched), and oxygen (white).

Bond valence sum analysis[30] reveals that in polyanion **1** the *trans*-related terminal ligands of the unique tungsten linker are arranged so that the water molecule is *external* [W19–O19T 2.27(2) Å] and the oxo ligand is *internal* [W19–O19N 1.72(2) Å], see Figure 1. This is in complete agreement with all other compounds containing the $[As_2W_{19}O_{67}(H_2O)]$ fragment, including the precursor itself.[11,13a,16] Interestingly, the situation is reversed for the dipalladium(II)-substituted $[Cs_2K(H_2O)_7Pd_2WO(H_2O)(A\text{-}\alpha\text{-}SiW_9O_{34})_2]^{9-}$ ($Pd_2Si_2W_{19}$) which our group reported very recently.[29] This species is composed of two (A-α-SiW_9O_{34}) Keggin moieties linked by a $WO(H_2O)$ group and two equivalent, square-planar Pd^{2+} ions, leading to a sandwich-type structure with C_{2v} symmetry. In $Pd_2Si_2W_{19}$, the central tungsten atom has the terminal oxo group in the *external* position, and the *trans*-related water molecule is pointing towards the inside of the central polyanion cavity. This observation allows for the conclusion that the two lone pairs of electrons associated with the As^{III} heteroatoms in **1** and **2** exhibit steric and electronic constraints which do not allow the existence of a long, *internal* $W–OH_2$ bond.

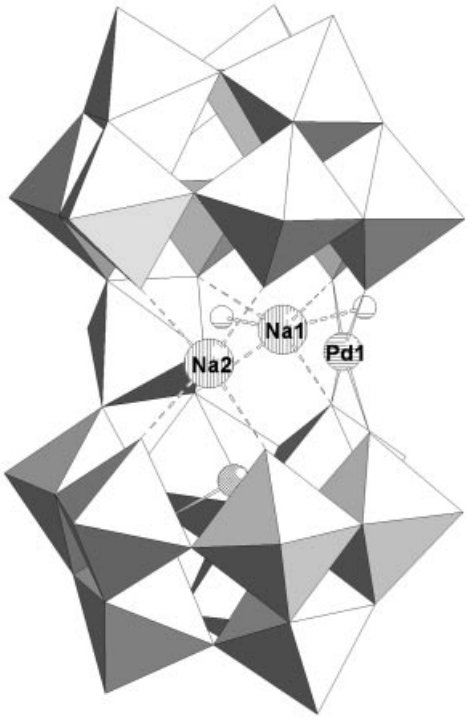

Figure 2. Combined polyhedral/ball and stick representation of **1**. The polyhedra represent WO_6 and the shading of the balls is as follows: arsenic (cross-hatched) and oxygen (white).

We also report on the tripalladium(II)-substituted, dimeric tungstoarsenate(III) $[Cs_2Na(H_2O)_8Pd_3(\alpha\text{-}AsW_9O_{33})_2]^{9-}$ (**2**), which has been synthesized by reaction of $PdCl_2$ with $Na_9[\alpha\text{-}AsW_9O_{33}]$ in aqueous acidic medium and isolated as a mixed cesium–sodium salt. Polyanion **2** is composed of two ($\alpha\text{-}AsW_9O_{33}$) units linked by three square-planar Pd^{2+} ions (see Figure 3). Therefore, **2** represents the arsenic(III) analog of $[Cs_2Na(H_2O)_{10}Pd_3(\alpha\text{-}SbW_9O_{33})_2]^{9-}$ ($Pd_3Sb_2W_{18}$), which we reported very recently.[28] Both of these tripalladium-substituted, sandwich-type species exhibit the same kind of bonding of the palladium atoms to the two Keggin fragments. Specifically, each palladium atom is bound to two oxo groups of the same W_3O_{13} triad of each Keggin unit. Interestingly, this is very different from the structurally related 3d transition-metal derivatives $[(M(H_2O)_3(\alpha\text{-}AsW_9O_{33})_2]^{9-}$ (M = Mn^{2+}, Co^{2+}, Ni^{2+}, Cu^{2+} and Zn^{2+}).[13] The latter exhibit transition-metal centers which are bound by two oxo groups of two different W_3O_{13} triads of each Keggin unit. We believe that the difference in the coordination geometry of the incorporated transition-metal center (square-planar for Pd^{II} versus square pyramidal for Cu^{II} or Zn^{II}) determines which bonding mode is preferred. It must be re-emphasized that this conclusion applies to tungstoarsenates(III). Interestingly, Krebs et al. observed a "non-eclipsed" bonding mode of the three palladium centers in $[Pd_3(TeW_9O_{33})_2]^{10-}$, which indicates that the type of heteroatom may also influence the bonding mode of the palladium ions to the two Keggin caps.[6]

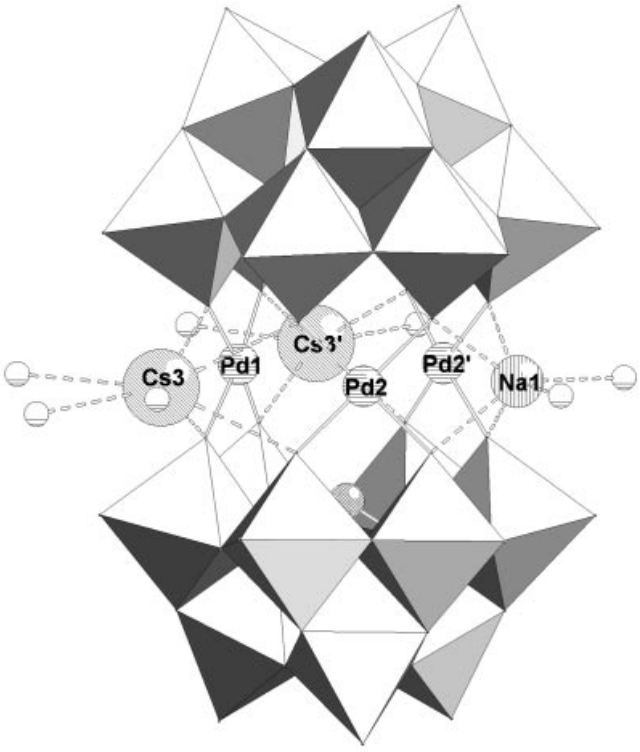

Figure 3. Combined polyhedral/ball and stick representation of $[Cs_2Na(H_2O)_8Pd_3(\alpha\text{-}AsW_9O_{33})_2]^{9-}$ (**2**) showing labels for the heavy atoms in the central belt. The polyhedra represent WO_6 and the shading of the remaining atoms is as follows: arsenic (cross-hatched) and oxygen (white).

The central belt of **2** is completed by two Cs^+ and a Na^+ ion, which occupy the vacancies between the adjacent palladium centers, resulting in a polyanion with idealized C_{2v} symmetry (see Figure 3). The two symmetry-equivalent cesium ions Cs3 and Cs3′ are coordinated to four oxo groups of **2** [Cs···O 3.065–3.168(13) Å] and three oxo groups of a neighboring polyanion [Cs···O 3.069–3.245(13) Å]. As expected, the sodium ion Na1 is six-coordinate and is bonded by four bridging oxo groups [Na1···O 2.448–2.449(16) Å] of **2** and two terminal water molecules [Na1···O 2.40(3) Å], resulting in an octahedral coordination sphere.

The synthetic procedure for **2** is very similar to that of $Pd_3Sb_2W_{18}$, which was prepared by interaction of $Pd(CH_3COO)_2$ with $Na_9[\alpha\text{-}SbW_9O_{33}]$.[28] Polyanion **2** was synthesized in good yield in a simple one-pot procedure by interaction of $PdCl_2$ with $Na_9[\alpha\text{-}AsW_9O_{33}]$ in aqueous acidic medium (pH 4.8). Interestingly, we have not been able to synthesize **2** using $Pd(CH_3COO)_2$ as a palladium source. In fact, reaction of $Pd(CH_3COO)_2$ with $Na_9[\alpha\text{-}AsW_9O_{33}]$ in aqueous acidic medium (pH 4.8) resulted in **1**. As described above, we were eventually able to identify a more rational synthetic procedure for **1** using the dilacunary precursor $[As_2W_{19}O_{67}(H_2O)]^{14-}$ (see also Experimental Section).

Nevertheless, it is somewhat surprising that the two pure, water soluble, commercially available palladium(II) salts $PdCl_2$ and $Pd(CH_3COO)_2$ react differently with the same lacunary polyoxoanion precursor $[\alpha\text{-}AsW_9O_{33}]^{9-}$, resulting in two different products **1** and **2**.

Electrochemistry

The instability of **1** precludes any interesting study of its electrochemical behavior on a well-defined species.

In contrast, **2** will increase the steadily expanding series of the very few Pd-containing heteropolyanions characterized by cyclic voltammetry. With the exception of $K_{12}[WZnPd^{II}_2(H_2O)_2(ZnW_9O_{34})_2]\cdot 38H_2O$, which was studied by Neumann et al.,[25a] and an allusion to the electrochemistry of $K_2Na_6[Pd_2W_{10}O_{36}]\cdot 22H_2O$,[26] only two polyanions $[Cs_2Na(H_2O)_{10}Pd_3(\alpha\text{-}SbW_9O_{33})_2]^{9-}$ ($Pd_3Sb_2W_{18}$)[28] and $[Cs_2K(H_2O)_7Pd_2WO(H_2O)(A\text{-}\alpha\text{-}SiW_9O_{34})_2]^{9-}$ ($Pd_2Si_2W_{19}$)[29] have been characterized to date by cyclic voltammetry. In the latter two examples, cyclic voltammetric studies show deposition of Pd^0 on the glassy carbon electrode surface, giving a film with a particularly well-behaved hydrogen sorption/desorption pattern.

In anticipation of future comparisons, essentially with its Sb-analog $Pd_3Sb_2W_{18}$,[28] polyanion **2** was studied by cyclic voltammetry in 0.4 M (CH_3COO^- + CH_3COOH) pH 5 buffer. Figure 4 shows the pattern observed for a 2×10^{-4} M solution of **2**. For a sequential description of the voltammogram in Figure 4, the potential domain can be divided into two parts. In the domain from –0.1 V to –0.520 V, the first broad cathodic peak observed roughly between –0.300 V and –0.360 V vs. SCE features the Pd^0 deposition process, which is ill-separated from the reduction of the W centers. This behavior is much the same as observed previously for the closely related $Pd_3Sb_2W_{18}$, but differs from that obtained for $PdSO_4$ solutions. With the present complex **2**, the second potential domain starting from –0.1 V to + 1.0 V in the positive potential direction and back to –0.1 V represents unambiguously the oxidation of the deposited Pd surface, followed by the reduction of the oxide. With $PdSO_4$, a broad drawn-out deposition wave was obtained, which is in agreement with the usual observation that the deposition can be performed in a large potential domain.[31] Whatever the Pd-containing compound, the subsequent, sharp cathodic peak with a sharp and narrow anodic counterpart features the hydrogen sorption/desorption processes. It is noteworthy that the film built from **2** shows the same remarkable hydrogen sorption/desorption characteristics obtained previously with $Pd_3Sb_2W_{18}$,[28] thus underscoring the excellent quality of the deposited film, compared with direct deposition from $PdSO_4$.

Typically, the potential cycling program in Figure 4 ensured that the deposition of Pd^0 on the electrode surface was restricted to the potential domain between + 0.2 V and –0.52 V. Alternatively, film deposition can be realized by potentiostatic electrolysis at –0.5 V. The rate at which the film became thicker increases with the more negative value of the potential selected for the cathodic end of the cyclic potential scan or, alternatively, with the more negative value chosen for controlled potential electrolysis. As expected, the

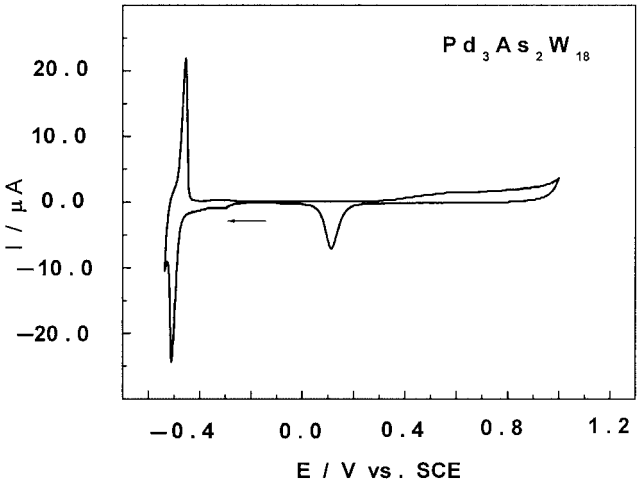

Figure 4. Representative cyclic voltammogram observed upon continuous cycling at a glassy carbon electrode of a 2×10^{-4} M solution of **2** in 0.4 M (CH_3COO^- + CH_3COOH) pH = 5 buffer. The potential variation was between –0.520 V and + 1.0 V. The arrow indicates the direction of the first scan, which starts at –0.1 V. Working electrode: glassy carbon; reference electrode: SCE; scan rate: 2 mV s^{-1}.

thickness increases also with the number of cycles or the duration of potentiostatic electrolysis. These observations parallel the literature results for Pd^0 deposition from ions in solution.[31] The domain starting from –0.1 V to + 1.0 V in the positive potential direction and back to –0.1 V represents unambiguously the oxidation of the deposited Pd surface, followed by reduction of the oxide. This part of the pattern is exactly the same as that obtained previously with $Pd_3Sb_2W_{18}$.[28]

The stability and robustness of the film deposited from **2** was tested in the following way. After deposition of a film on the glassy carbon surface, the electrode was taken out of the solution, copiously rinsed with Millipore water, left for some time in the open air, and then soaked in pure supporting electrolyte (pH = 5). The pattern obtained in Figure 4 is exactly reproduced, except for the broad "first" deposition wave which is missing. This pattern could be cycled several times without observing any changes. This experiment demonstrates the perfect stability of the film. A rough estimate of the film thickness in Figure 4 can be calculated. Typically, the building of the film shown in Figure 4 necessitates 263×10^{-6} C, which corresponds to about 1.3×10^{15} Pd atoms. With an atomic radius of 140 pm for Pd,[32] a monolayer of these atoms would cover an area of 8.1×10^{-5} m^2. With an electrode surface area of 7.07×10^{-6} m^2, the deposited film corresponds to about eleven monolayers.

In short, results gathered from the pertinent literature[31] suggest that Figure 4 features the characteristics of the deposition behavior of Pd^0 on the glassy carbon electrode surface. As a complementary cross-check, we were interested in verifying whether these surfaces display the electrocatalytic behavior that is usually expected for Pd^0 films. The electrocatalytic reduction of dioxygen was studied for this purpose. Figure 5 shows the superposition of the voltammograms obtained with the deposited Pd^0 film in the pure pH 5 electrolyte, and after bubbling air and pure dioxygen, separately, through the solution. It must be noted that no reduction of dioxygen occurred on the glassy carbon surface alone in the potential domain explored.[33] In contrast, a very efficient reduction of dioxygen was observed on the Pd^0-modified surface as can be inferred from the relatively positive potential location of the process. The catalytic process was efficient enough for the voltammograms to be polarogram-shaped. Furthermore, the plateau currents scale up roughly with the concentration of dioxygen in solution. Typically, a thin Pd^0 film comprising roughly six monolayers was used for the experiments shown in Figure 5. Actually, several film thicknesses were used, and a very efficient dioxygen reduction process was observed no matter what the film thickness. Finally, prolonged cycling of these electrodes in the presence of dioxygen did not induce any deactivation of the surfaces.

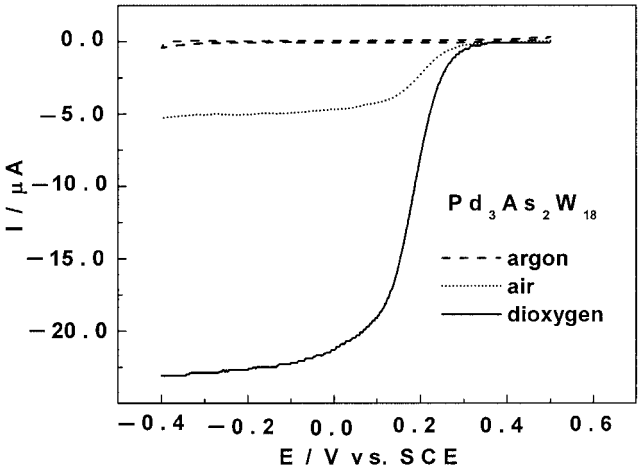

Figure 5. Cyclic voltammetry characterization, in 0.4 M (CH_3COO^- + CH_3COOH) pH = 5 buffer, of the electrocatalytic reduction of dioxygen on a thin film of Pd^0 (6 monolayers) deposited by **2** on a glassy carbon electrode; reference electrode: SCE; scan rate: 2 mV s^{-1}. The polarogram-shaped cyclic voltammograms were obtained with the Pd^0 film in pure supporting electrolyte deaerated with argon after air and pure dioxygen were bubbled, separately, through the solution.

Conclusions

We have synthesized the novel monopalladium(II)-substituted $[Na_2(H_2O)_2PdWO(H_2O)(\alpha\text{-}AsW_9O_{33})_2]^{10-}$ (**1**) and the tripalladium(II)-substituted $[Cs_2Na(H_2O)_8Pd_3(\alpha\text{-}AsW_9O_{33})_2]^{9-}$ (**2**). These polyanions represent the first examples of structurally characterized palladium(II)-substituted tungstoarsenates(III). Both **1** and **2** were prepared in simple, one-pot procedures by reaction of Pd^{2+} ions with $[As_2W_{19}O_{67}(H_2O)]^{14-}$ and $[\alpha\text{-}AsW_9O_{33}]^{9-}$, respectively, in aqueous acidic medium (pH 4.8). Polyanion **2** represents the arsenic(III) analog of $[Cs_2Na(H_2O)_{10}Pd_3(\alpha\text{-}SbW_9O_{33})_2]^{9-}$ ($Pd_3Sb_2W_{18}$), and it is also stable in a large pH domain (pH 0–5). Polyanion **1** is much less stable in solution, which can be rationally explained by structural considerations. The

backbone of **1** is composed of two $[\alpha\text{-}AsW_9O_{33}]^{9-}$ fragments connected by a $WO(H_2O)^{4+}$ unit, which represents the well-known $[As_2W_{19}O_{67}(H_2O)]^{14-}$ fragment. However, **1** has only one palladium(II) center incorporated rather than the expected two, and furthermore, this polyanion exhibits an additional, highly unusual feature: the third addenda atom position in the central belt of **1** is occupied by a sodium ion. This is completely unprecedented for this structural subclass of polyanions and probably explains the low stability of **1** in solution. In fact, polyanion **1** could be considered as a monolacunary species, and it also appears like an intermediate in the formation of the hypothetical dipalladium(II)-substituted $[Pd_2WO(H_2O)(\alpha\text{-}AsW_9O_{33})_2]^{10-}$, which we have not been able to isolate to date. Furthermore, our synthetic work in this direction is aimed at the synthesis of the antimony(III) analog of **1** with the suggested formula $[Na_2(H_2O)_2PdWO(H_2O)(\alpha\text{-}SbW_9O_{33})_2]^{10-}$and of the dipalladium tungstoantimonate(III) $[Pd_2WO(H_2O)(\alpha\text{-}SbW_9O_{33})_2]^{10-}$.

Both polyanions **1** and **2** were electrochemically investigated, but the low stability of **1** in the aqueous solutions tested in this work precluded a reliable study. On the other hand, cyclic voltammetry of **2** in a pH 5 medium resulted in the deposition of a Pd^0 film on the glassy carbon electrode surface. The voltammogram showed a particularly sharp hydrogen sorption/desorption as observed previously with the closely related $Pd_3Sb_2W_{18}$. The glassy carbon surface modified by deposition of Pd^0 from **2** proved to be stable and remarkably efficient for the electrocatalytic reduction of dioxygen, at least in the pH 5 medium used here.

Experimental Section

Synthesis

The polyanion precursors $Na_9[\alpha\text{-}AsW_9O_{33}]$ and $K_{14}[As_2W_{19}O_{67}(H_2O)]$ were synthesized according to the published procedures.[8a,11] The identity of the products was confirmed by infrared spectroscopy. All other reagents were used as purchased without further purification.

$Cs_3Na_7[Na_2(H_2O)_2PdWO(H_2O)(\alpha\text{-}AsW_9O_{33})_2]\cdot 1.5NaCl\cdot 22H_2O$ (1a): A sample of $PdCl_2$ (0.040 g, 0.23 mmol) was dissolved in NaAc buffer (20 mL of 0.5 M solution, pH 4.8) while stirring. $K_{14}[As_2W_{19}O_{67}(H_2O)]$ (0.50 g, 0.095 mmol) was then added. The solution was heated to 80 °C for about 1 h and filtered after it had cooled, and then CsCl (0.5 mL of 1.0 M solution) was added to the red filtrate. Slow evaporation at room temperature led to 0.34 g (yield 60%) of a red crystalline product after about two weeks. IR: 944 (m), 893 (s), 796 (s), 746 (vs), 608 (w), 503 (w), 462 (w), 435 (w) cm^{-1}. **1a**: calcd. As 2.5, Cl 0.9, Cs 6.7, Na 4.1, Pd 1.8, W 58.6; found As 2.3, Cl 0.6, Cs 6.7, Na 3.8, Pd 1.5, W 57.7.

$Cs_3Na_6[Cs_2Na(H_2O)_8Pd_3(\alpha\text{-}AsW_9O_{33})_2]\cdot NaCl\cdot 15H_2O$ (2a): A sample of $PdCl_2$ (0.06 g, 0.34 mmol) was dissolved in NaAc buffer (20 mL of 0.5 M solution, pH 4.8) while stirring. $Na_9[\alpha\text{-}AsW_9O_{33}]$ (0.50 g, 0.20 mmol) was then added. The solution was heated to 80 °C for about 1 h and filtered after it had cooled, and then CsCl (0.5 mL of 1.0 M solution) was added to the red filtrate. Slow evaporation at room temperature led to 0.30 g (yield 49%) of a brown crystalline product after about two weeks. IR: 955 (sh), 938 (m), 897 (m), 860 (sh), 782 (vs), 730 (m), 685 (m), 516 (w), 483 (w), 448 (w) cm^{-1}. **2a**: calcd. As 2.4, Cl 0.6, Cs 10.8, Na 3.0, Pd 5.2, W 54.0; found As 2.5, Cl 0.5, Cs 10.4, Na 2.8, Pd 4.7, W 54.9.

All elemental analyses were performed by Kanti Labs Ltd. in Mississauga, Canada. The IR spectra were recorded with a Nicolet Avatar FTIR spectrophotometer in KBr pellets.

X-ray Crystallography

A crystal of **1a** was mounted on a glass fiber for indexing and to collect intensity data at 200 K on a Bruker D8 SMART APEX CCD single-crystal diffractometer using Mo-K_α radiation (λ = 0.71073 Å). Direct methods were used to solve the structure and to locate the heavy atoms (SHELXS97). The remaining atoms were then found from successive difference maps (SHELXL97). The final cycle of refinement, including the atomic coordinates, anisotropic thermal parameters (all W, Pd, Cs, Na, As, Cl atoms) and isotropic thermal parameters (all O atoms) converged at $R = 0.102$ and $R_w = 0.230$ [$I > 2\sigma(I)$]. No hydrogen atoms were included in the refinement. In the final difference map, the deepest hole was –10.945 e Å^{-3} and the highest peak 9.592 e Å^{-3}. The residual electron density is located exclusively near the tungsten atoms. Routine Lorentz and polarization corrections were applied and an absorption correction was performed using the SADABS program.[34]

A crystal of compound **2a** was mounted on a glass fiber for indexing and to collect intensity data at 150 K on a Rigaku Saturn 70 CCD single-crystal diffractometer using Mo-K_α radiation (λ = 0.71070 Å). Direct methods were used to solve the structure and to locate the heavy atoms (SHELXS97). The remaining atoms were then found from successive difference maps (SHELXL97). The final cycle of refinement, including the atomic coordinates, anisotropic thermal parameters (all W, Pd, Cs, Na, As, Cl atoms) and isotropic thermal parameters (all O atoms) converged at $R = 0.080$ and $R_w = 0.216$ [$I > 2\sigma(I)$]. No hydrogen atoms were included in the refinement. In the final difference map, the deepest hole was –7.319 e Å^{-3} and the highest peak 5.813 e Å^{-3}. Routine Lorentz and polarization corrections were applied and an absorption correction was performed using the MULTISCAN program.[35] Crystallographic data for **1a** and **2a** are summarized in Table 1.

Further details of the crystal-structure investigations may be obtained from the Fachinformationszentrum Karlsruhe, 76344 Eggenstein-Leopoldshafen, Germany, on quoting the depository numbers CSD-415125 (**1a**) and CSD-415128 (**2a**).

Electrochemistry

General Methods and Materials: Pure water was used throughout. It was obtained by passing through a RiOs 8 unit followed by a Millipore-Q Academic purification set. All reagents were of high-purity grade and were used as purchased without further purification. The UV/Visible spectra were recorded on a Perkin–Elmer Lambda 19 spectrophotometer with 2×10^{-5} M solutions of the relevant polyanion. Matched 1.000 cm optical path quartz cuvettes were used. The compositions of the various media were as follows: for pH 0: HCl or H_2SO_4; for pH 1 to 3: 0.2 M Na_2SO_4 + H_2SO_4; for pH 4 and 5: 0.4 M CH_3COONa + CH_3COOH; for pH 6 and 7: 0.4 M NaH_2PO_4 + NaOH.

Electrochemical Experiments: The same media as those used for UV/Visible spectroscopy were used for the electrochemical investigation, but the polyanion concentration was 2×10^{-4} M. The solutions were deaerated thoroughly for at least 30 min with pure argon and kept under a positive pressure of this gas during the experiments. All cyclic voltammograms were recorded at a scan rate of 2 mV s^{-1}, unless otherwise stated. The source, mounting, and polishing of the glassy carbon (GC, Tokai, Japan) electrodes has been

Table 1. Crystal data and structure refinement for $Cs_3Na_7[Na_2(H_2O)_2PdWO(H_2O)(\alpha\text{-}AsW_9O_{33})_2]\cdot 1.5NaCl\cdot 22H_2O$ (**1a**) and $Cs_3Na_6[Cs_2Na(H_2O)_8Pd_3(\alpha\text{-}AsW_9O_{33})_2]\cdot NaCl\cdot 15H_2O$ (**2a**).

	1a	**2a**
Formula	$As_2Cl_{1.5}Cs_3H_{50}Na_{10.5}O_{92}PdW_{19}$	$As_2ClCs_5H_{46}Na_8O_{89}Pd_3W_{18}$
M_w [g mol^{-1}]	5965.2	6132.7
Crystal color	Red-brown	Brown
Crystal system	Triclinic	Monoclinic
Crystal size [mm]	0.20 × 0.04 × 0.02	0.18 × 0.06 × 0.03
Space group (No.)	$P\bar{1}$ (2)	$P2_1/m$ (11)
a [Å]	13.2465(16)	13.1842(5)
b [Å]	16.873(2)	19.6584(7)
c [Å]	23.080(3)	18.2377(6)
α [°]	107.315(2)	
β [°]	95.025(3)	100.7660(10)
γ [°]	98.040(3)	
Volume [Å^3]	4830.6(10)	4643.7(3)
Z	2	2
$d_{calcd.}$ [mg m^{-3}]	4.02	4.22
abs. coeff. [mm^{-1}]	24.677	25.353
Reflections (unique)	23941	22880
Reflections (obs.)	18754	17760
R [$I > 2\sigma(I)$][a]	0.102	0.080
R_w (all data)[b]	0.230	0.216
Diff. Peak [e Å^{-3}]	9.592	5.813
Diff. Hole [e Å^{-3}]	–10.945	–7.319

[a] $R = \Sigma||F_o| - |F_c||/\Sigma|F_o|$. [b] $R_w = [\Sigma w(F_o^2 - F_c^2)^2/\Sigma w(F_o^2)^2]^{1/2}$.

described before.[36] The glassy carbon samples had a diameter of 3 mm. The electrochemical set-up was an EG & G 273 A driven by a PC with the M270 software. Potentials are quoted against a saturated calomel electrode (SCE). The counter electrode was platinum gauze with a large surface area. All experiments were performed at room temperature.

Stability Studies: We tried to identify conditions at which polyanions **1** and **2** were stable enough to allow for electrochemical studies. For this purpose, the UV/Vis spectrum of each compound was monitored as a function of pH over a period of at least 24 h at room temperature. This delay was selected as a compromise between the time needed for electrochemical characterization of the complexes and that for eventual long-lasting or preparative-scale catalytic or electrocatalytic processes. Only spectra reproducible with respect to shape, absorbance, and wavelength location over this period of time were considered to indicate complete stability. At these conditions, **2** shows complete stability from pH 0 through to 5. It is interesting to compare this stability domain to that of the closely related polyanion $Pd_3Sb_2W_{18}$, which is stable from pH 0 to 7.[28] Provisionally, this difference might be attributed to the different heteroatoms Sb versus As. A complementary cross-check of these suggested stabilities was obtained by electrochemical experiments: the complete voltammetric study for each pH value lasts, typically, between 8 and 10 h. Perfect reproducibility of the voltammogram obtained for a selected potential scan rate was observed and taken as a complementary criterion of stability. In contrast to the behavior of **2**, no satisfactory stability domain could be determined for **1** in aqueous solution, despite efforts to modify the composition of the supporting electrolytes.

Acknowledgments

U.K. thanks the International University Bremen for research support and the Florida State University Chemistry Department for unlimited access to the single-crystal X-ray diffractometer. B.K. and L.N. thank the University Paris Sud XI and the CNRS (UMR 8000) for research support. Figures 1–3 were generated by Diamond Version 3.0d (copyright Crystal Impact GbR).

[1] *Chemical Reviews, Polyoxometalates* (Ed.: C. L. Hill), **1998**.
[2] M. T. Pope, *Heteropoly and Isopoly Oxometalates*, Springer-Verlag: Berlin, **1983**.
[3] M. T. Pope, A. Müller, *Angew. Chem. Int. Ed.* **1991**, *30*, 34–48.
[4] M. T. Pope, *Comp. Coord. Chem. II* **2003**, *4*, 635–677.
[5] *Polyoxometalates: From Platonic Solids to Anti-Retroviral Activity* (Eds.: M. T. Pope, A. Müller), Kluwer, Dordrecht, The Netherlands, **1994**.
[6] *Polyoxometalate Chemistry: From Topology via Self-Assembly to Applications* (Eds.: M. T. Pope, A. Müller), Kluwer, Dordrecht, The Netherlands, **2001**.
[7] *Polyoxometalate Chemistry for Nano-Composite Design* (Eds.: T. Yamase, M. T. Pope), Kluwer, Dordrecht, The Netherlands, **2002**.
[8] a) C. Tourné, A. Revel, G. Tourné, M. Vendrell, *C. R. Hebd. Seances Acad. Sci. Ser. C* **1973**, *277*, 643–645; b) M. Leyrie, J. Martin-Frére, G. Hervé, *C. R. Hebd. Seances Acad. Sci. Ser. C* **1974**, *279*, 895–897; c) M. Leyrie, G. Hervé, *Nouv. J. Chim.* **1978**, *2*, 233–237.
[9] a) F. Robert, M. Leyrie, G. Hervé, A. Tézé, Y. Jeannin, *Inorg. Chem.* **1980**, *19*, 1746–1752; b) Y. Jeannin, *C. R. Acad. Sci. Ser. IIc* **2000**, *3*, 295–299; c) Y. Jeannin, J. Martin-Frère, *Inorg. Chem.* **1979**, *18*, 3010–3014; d) M. Leyrie, A. Tézé, G. Hervé, *Inorg. Chem.* **1985**, *24*, 1275–1277.
[10] K. Wassermann, M. H. Dickman, M. T. Pope, *Angew. Chem. Int. Ed.* **1997**, *36*, 1445–1448.
[11] U. Kortz, M. G. Savelieff, B. S. Bassil, M. H. Dickman, *Angew. Chem. Int. Ed.* **2001**, *40*, 3384–3386.
[12] F. Robert, M. Leyrie, G. Hervé, *Acta Crystallogr. Sect. B* **1982**, *38*, 358–362.
[13] a) U. Kortz, N. K. Al-Kassem, M. G. Savelieff, N. A. Al Kadi, M. Sadakane, *Inorg. Chem.* **2001**, *40*, 4742–4749; b) P. Mialane, J. Marrot, E. Rivière, J. Nebout, G. Hervé, *Inorg. Chem.* **2001**, *40*, 44–48.
[14] U. Kortz, S. Nellutla, A. C. Stowe, N. S. Dalal, J. van Tol, B. S. Bassil, *Inorg. Chem.* **2004**, *43*, 144–154.

[15] U. Kortz, M. G. Savelieff, B. S. Bassil, B. Keita, L. Nadjo, *Inorg. Chem.* **2002**, *41*, 783–789.
[16] a) C. Tourné, G. Tourné, *C. R. Acad. Sci. Paris Ser. C* **1975**, *281*, 933–936; b) L. G. Detusheva, L. I. Kuznetsova, V. A. Likholobov, A. A. Vlasov, N. N. Boldyreva, S. G. Poryvaev, V. V. Malakhov, *Russ. J. Coord. Chem.* **1999**, *25*, 569–575; c) P. Mialane, J. Marrot, A. Mallard, G. Hervé, *Inorg. Chim. Acta* **2002**, *328*, 81–86.
[17] F. Lefebvre, M. Leyrie, G. Hervé, C. Sanchez, J. Livage, *Inorg. Chim. Acta* **1983**, *73*, 173–178.
[18] U. Kortz, C. Holzapfel, M. Reicke, *J. Mol. Struct.* **2003**, *656*, 93–100.
[19] Y. Jeannin, J. Martin-Frère, *J. Am. Chem. Soc.* **1981**, *103*, 1664–1667.
[20] G. Sazani, M. H. Dickman, M. T. Pope, *Inorg. Chem.* **2000**, *39*, 939–943.
[21] F. Hussain, U. Kortz, R. J. Clark, *Inorg. Chem.* **2004**, *43*, 3237–3241.
[22] F. Hussain, M. Reicke, U. Kortz, *Eur. J. Inorg. Chem.* **2004**, 2733–2738.
[23] W. H. Knoth, P. J. Domaille, R. L. Harlow, *Inorg. Chem.* **1986**, *25*, 1577–1584.
[24] C. M. Tourné, G. F. Tourné, F. Zonnevijlle, *J. Chem. Soc. Dalton Trans.* **1991**, 143–155.
[25] a) R. Neumann, A. M. Khenkin, *Inorg. Chem.* **1995**, *34*, 5753–5760; b) R. Neumann, A. M. Khenkin, D. Juwiler, H. Miller, M. Gara, *J. Mol. Catal A-Chem.* **1997**, *117*, 169–183; c) U. Schuchardt, D. Cardoso, R. Sercheli, R. Pereira, R. S. da Cruz, M. C. Guerreiro, D. Mandelli, E. V. Spinace, E. L. Fires, *Appl. Catal. A-Gen.* **2001**, *211*, 1–17; d) V. Kogan, Z. Aizenshtat, R. Neumann, *New J. Chem.* **2002**, *26*, 272–274; e) W. Adam, P. L. Alsters, R. Neumann, C. R. Saha-Moller, D. Seebach, A. K. Beck, R. Zhang, *J. Org. Chem.* **2003**, *68*, 8222–8231; f) W. Adam, P. L. Alsters, R. Neumann, C. R. Saha-Moller, D. Sloboda-Rozner, R. Zhang, *J. Org. Chem.* **2003**, *68*, 1721–1728.
[26] S. J. Angus-Dunne, R. C. Burns, D. C. Craig, G. A. Lawrance, *J. Chem. Soc. Chem. Commun.* **1994**, 523–524.
[27] a) L. Bi, F. Hussain, U. Kortz, M. Sadakane, M. H. Dickman, *Chem. Commun.* **2004**, 1420–1421; b) L.-H. Bi, U. Kortz, B. Keita, L. Nadjo, *Dalton Trans.* **2004**, 3184–3190.
[28] L.-H. Bi, M. Reicke, U. Kortz, B. Keita, L. Nadjo, R. J. Clark, *Inorg. Chem.* **2004**, *43*, 3915–3920.
[29] L.-H. Bi, U. Kortz, B. Keita, L. Nadjo, H. Borrmann, *Inorg. Chem.* **2004**, *43*, 8367–8372.
[30] I. D. Brown, D. Altermatt, *Acta Crystallogr. Sect. B* **1985**, *41*, 244–247.
[31] Representative papers on Pd^0 deposition from Pd^{2+} solutions and its electrochemical behaviour include: a) K.-H. Lubert, M. Guttmann, L. Beyer, *J. Electroanal. Chem.* **1999**, *462*, 174–180; b) K.-H. Lubert, M. Guttmann, L. Beyer, K. Kalcher, *Electrochem. Commun.* **2001**, *3*, 102–106; c) X.-G. Zhang, T. Arikawa, Y. Murakami, K. Yahikozawa, Y. Takasu, *Electrochimica Acta* **1995**, *40*, 1889–1897; d) M. J. Ball, C. A. Lucas, N. M. Markovic, V. Stamenkovic, P. N. Ross, *Surface Sci.* **2002**, *518*, 201–209; e) X.-Q. Tong, M. Aindow, J. P. G. Farr, *J. Electroanal. Chem.* **1995**, *395*, 117–126; f) N. Tateishi, K. Yahikozawa, K. Nashimura, M. Suzuki, Y. Iwanaga, M. Watanabe, E. Enami, Y. Matsuda, Y. Takasu, *Electrochimica Acta* **1991**, *36*, 1235–1240; g) X-G. Zhang, Y. Murakami, K. Yahikozawa, Y. Takasu, *Electrochimica Acta* **1997**, *42*, 223–227; h) N. M. Markovic, C. A. Lucas, V. Climent, V. Stamenkovic, P. N. Ross, *Surface Sci.* **2000**, *465*, 103–114; i) L-J. Wan, T. Suzuki, K. Sashikata, J. Okada, J. Inukai, K. Itaya, *J. Electroanal. Chem.* **2000**, *484*, 189–193; j) A. M. El-Aziz, L. A. Kibler, D. M. Kolb, *Electrochem. Commun.* **2002**, *4*, 535–539; k) M. Arenz, V. Stamenkovic, T. J. Schmidt, K. Wandelt, P. N. Ross, N. M. Markovic, *Surface Sci.* **2003**, *523*, 199–209; l) A. Hernandez Creus, Y. Gimeno, P. Diaz, L. Vazquez, S. Gonzalez, R. C. Salvarezza, A. J. Arvia, *J. Phys. Chem. B* **2004**, *108*, 10785–10795.
[32] Landoldt-Börnstein, I. Band, *Atom- und Molekularphysik, 4. Teil: Kristalle*, 6th ed., Springer, Berlin, **1955**, p. 527.
[33] B. Keita, M. Benaïssa, L. Nadjo, R. Contant, *Electrochem. Commun.* **2002**, *4*, 663–668.
[34] G. M. Sheldrick, *SADABS*; University of Göttingen, **1996**.
[35] R. H. Blessing, *Acta Crystallogr. Sect. A* **1995**, *51*, 33–38.
[36] B. Keita, F. Girard, L. Nadjo, R. Contant, R. Belghiche, M. Abbessi, *J. Electroanal. Chem.* **2001**, *508*, 70–80.

Received: February 11, 2005
Published Online: June 21, 2005

